© 2014. Published by The Company of Biologists Ltd | The Journal of Experimental Biology (2014) 217, 4079-4090 doi:10.1242/jeb.112391

RESEARCH ARTICLE

Encoding wide-field motion and direction in the central complex of the cockroach *Blaberus discoidalis*

Nicholas D. Kathman*, Malavika Kesavan and Roy E. Ritzmann

ABSTRACT

In the arthropod brain, the central complex (CX) receives various forms of sensory signals and is associated with motor functions, but its precise role in behavior is controversial. The optomotor response is a highly conserved turning behavior directed by visual motion. In tethered cockroaches, 20% procaine injected into the CX reversibly blocked this behavior. We then used multichannel extracellular recording to sample unit activity in the CX in response to wide-field visual motion stimuli, moving either horizontally or vertically at various temporal frequencies. For the 401 units we sampled, we identified five stereotyped response patterns: tonically inhibited or excited responses during motion, phasically inhibited or excited responses at the initiation of motion, and phasically excited responses at the termination of motion. Sixty-seven percent of the units responded to horizontal motion, while only 19% responded to vertical motion. Thirty-eight percent of responding units were directionally selective to horizontal motion. Response type and directional selectivity were sometimes conditional with other stimulus parameters, such as temporal frequency. For instance, 16% of the units that responded tonically to low temporal frequencies responded phasically to high temporal frequencies. In addition, we found that 26% of wide-field motion responding units showed a periodic response that was entrained to the temporal frequency of the stimulus. Our results show a diverse population of neurons within the CX that are variably tuned to wide-field motion parameters. Our behavioral data further suggest that such CX activity is required for effective optomotor responses.

KEY WORDS: Central complex, Insect brain, Multi-unit recording, Optomotor response, Wide-field motion

INTRODUCTION

Motor control can be complex, requiring input from many sources within the central nervous system of an animal. Local reflexes and pattern generators in thoracic ganglia of arthropods or spinal cords of vertebrates provide local control to motor neurons. Sensory receptors, including visual, tactile and chemosensors, monitor surroundings and lead to descending commands. Information from many of those sensors is processed through primary sensory systems and that processed information leads to descending commands that interact with the local control centers. As direct as this pathway seems, many behaviors also involve association areas of the brain. In insects, these include the mushroom bodies and central complex (Strausfeld, 2012). The manner in which these regions are involved in motor control, as well as the sensory information that is encoded in them, is an open question in neuroethology.

Case Western Reserve University, 10900 Euclid Avenue, Cleveland, OH 44106, USA.

*Author for correspondence (nick.kathman@gmail.com)

Received 8 August 2014; Accepted 22 September 2014

The central complex (CX) is a group of mid-line neuropils found in the insect brain. Some variant of this structure is found in all arthropods and some annelids with bilateral appendages (Strausfeld, 1999; Strausfeld, 2012). Cells of the CX receive input from various sensory modalities, including visual and tactile antennal information (Ritzmann et al., 2008; Pfeiffer and Homberg, 2014). The CX consists of five structures: the fan-shaped body (FB; also referred to as the upper division of the central body), ellipsoid body (EB; or lower division of the central body), the protocerebral bridge (PB) and a pair of noduli (Pfeiffer and Homberg, 2014).

Evidence from lesioning (Huber, 1960) and electrical stimulation (Otto, 1971) has long implicated the CX in regulating behavioral activities. More recently, neurogenetics have been used to disrupt the CX in *Drosophila* and show evidence for its role in many visually directed behaviors, such as orientation, gap climbing and visually-directed walking (Bausenwein et al., 1994; Strauss, 2002; Poeck et al., 2008; Kahsai et al., 2010; Triphan et al., 2010). Behavior has also been shown to modulate visual motion responses of CX neurons (Seelig and Jayaraman, 2013; Weir et al., 2014). In addition, the CX has been shown to be necessary for visually mediated place learning in insects (Ofstad et al., 2011).

In the cockroach, *Blaberus discoidalis*, further lesion studies have implicated the CX in forward walking, turning, climbing and tunnelling (Ridgel et al., 2007; Harley and Ritzmann, 2010). Moreover, extracellular neural activity recorded in the CX has been correlated with walking speed, turning direction and climbing (Bender et al., 2010; Guo and Ritzmann, 2013; Guo et al., 2014). Stimulating the CX was also found to invoke behaviors such as turning, where the direction of the turn was predicted by the stimulus location (Guo and Ritzmann, 2013).

The CX has also been shown to play a role in visual sensory processing. Extensive work has been done characterizing CX cells anatomically in relation to their role in polarized light vision in locusts, crickets and monarch butterflies (Sakura et al., 2008; Heinze and Reppert, 2011; Pfeiffer and Homberg, 2014). Intracellular recordings of CX neurons reveal representations of various types of visual motion in CX neurons of various insects, indicating directional preference (Phillips-Portillo, 2012) (flesh fly), and looming sensitivity (Rosner and Homberg, 2013) (locust). Two-photon calcium imaging in fruit flies has shown that ring neurons in the EB display directionally selective orientation tuning to narrow features that are arranged retinotopically with respect to their receptive fields (Seelig and Jayaraman, 2013).

Questions remain about the range of the visual response properties for CX neurons, especially relative to particular behaviors such as optomotor response and spatial orientation. The optomotor response is an orientation behavior in response to rotating wide-field motion (Borst et al., 2010) and is found in the cockroach (Szczecinski et al., 2014). Although the necessary directional motion is characterized in visual lobes (Borst and Haag, 2002; Borst et al., 2010), it is possible that the complete behavior could involve

The Journal of Experimental Biology (2014) doi:10.1242/jeb.112391

associative regions such as the CX. In this study, we first established that a functional CX is critical for the optomotor response by silencing CX activity with procaine. We then used multi-channel recording to monitor groups of CX neurons while presenting the cockroach with a wide range of repeated visual motion parameters, and thereby established ranges of response properties that are relevant to optomotor and other visually directed behaviors.

RESULTS

Silencing neurons of the central complex reduces optomotor response

In order to establish behavioral relevancy to the visual responses we recorded in the CX, we first observed the cockroach optomotor response. Seventy-five percent of untreated cockroaches walking on an air-suspended ball responded in a directional manner to right and left moving stripe patterns in their visual field (Fig. 1A). A 20% solution of the local anesthetic, procaine, injected into the CX reversibly blocked this response (Fig. 1B). The location of the injection site was determined by histological identification of dextran fluorescein that was mixed with the procaine. To control for general effects of fluid injection, we compared the procaine trials with insects that had been injected with saline solution. A significant reduction in the number of subjects that responded to optomotor stimuli was found in initial trials and trials taken 15 min after injection (χ^2 test, $P<0.05$). At 30 min and beyond, subjects performed normal optomotor responses. A 10% procaine solution only reduced the response at the initial testing time (Fig. 1B).

To control for additional effects of the surgery, we performed sham trials, where the insect's brain was exposed but with no injection. These trials showed no effect on optomotor response. Animals were also still able to walk after procaine injection. To verify that procaine-injected animals were not simply paralysed we measured general activity levels of each animal during drug trials and compared them with saline-injected animals. We found no significant difference between the groups at any time after injection (two-sample *t*-test, $P<0.05$) (supplementary material Table S1).

To verify that the procaine effectively blocked neural activity near the injection site, we performed seven multi-channel recordings in and outside of the CX during a procaine injection. Most, if not all, units recorded in or next to the CX were completely silenced (Fig. 1C). As with the behavioral trials, all units silenced by the drug were affected almost immediately (0.2±0.4 min from injection, mean ± s.d.) then recovered 10±5 min after injection (mean of four animals, 42 units), with some silencing lasting over 20 min (Fig. 1C). Recordings taken from regions distinctly outside of the CX showed little to no effects from procaine injected within the CX (Fig. 1D). These patterns were consistent in all seven recordings that were performed.

Wide-field visual motion and the central complex

Extracellular multichannel activity was recorded within or on the margins of the central complex of 14 insects. These recordings yielded a total of 401 units separated from the multi-unit activity. Units were sampled from both the FB and EB, sampling across most of the dorsal–ventral plane of the CX, with a large proportion of the recording sites located near the margins of the CX (Fig. 2D).

A series of 4 s visual stimulus trials (Fig. 2A,B) was presented to each animal in random order. Unit activity was monitored while the stripe field shifted for that trial. The stimulus for any given trial was either horizontal or vertical motion, shifting among 10 temporal frequencies between 0.25 and 5 Hz. Each parameter combination was replicated randomly 15–20 times over a period of 2–3 h.

Response types to wide-field motion

Our analysis of the resulting data followed several stages that led to ever more precise indications of the temporal properties of each response. First, we identified general responses as mean changes in firing rate, over all 15–20 trials, which were at least two standard deviations from their baseline firing rates between the beginning of motion and 500 ms after motion cessation. Responses were found for all units to each parameter combination. This analysis identified 268 of 401 units (67%) that consistently responded in some way to visual motion.

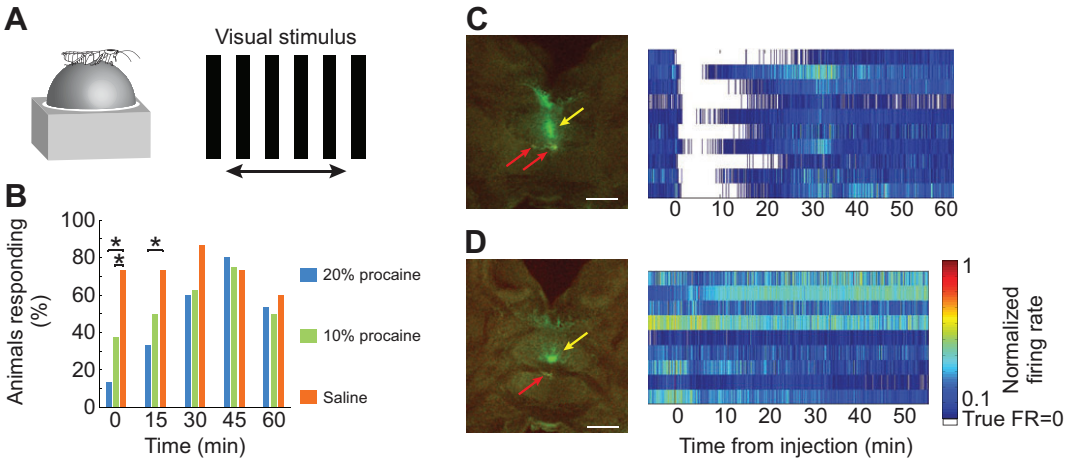

Fig. 1. Optomotor response is reduced after administration of local anesthetic in the central complex. (A) Turning response of *Blaberus discoidalis* to shifting stripes was measured while the insect was tethered to an air-supported Styrofoam ball. (B) Proportions of animals with a successful optomotor response at 15 min time intervals after the injection of 20% procaine (blue), 10% procaine (green) or saline (orange) into the CX (*N*=15, 16 and 15 animals, respectively). Both treatments were significantly different (χ^2 test, $P<0.05$) from saline controls at 0 min and only the 20% procaine was reduced at 15 min (*). This effect was reversed from 30 min on for both treatments. (C,D) Unit recordings during procaine injection verify that procaine did inactivate neural activity near the injection site, but not in regions of the brain outside the CX. Activity of units recorded from the margin (C) and outside (D) the CX, before and after procaine injection (*t*=0), is depicted by heatmaps of normalized firing rate (FR) of all units (rows) from the tetrode locations indicated in the image to the left (red arrow). Unit silence (when true instantaneous firing rate is 0) is indicated as white in the heatmaps. Green dye seen in the confocal images (yellow arrow) was injected along with the procaine. A clear gap exists between the procaine and the recording site in D, but not in C. Scale bars: 200 µm.

The Journal of Experimental Biology

The Journal of Experimental Biology (2014) doi:10.1242/jeb.112391

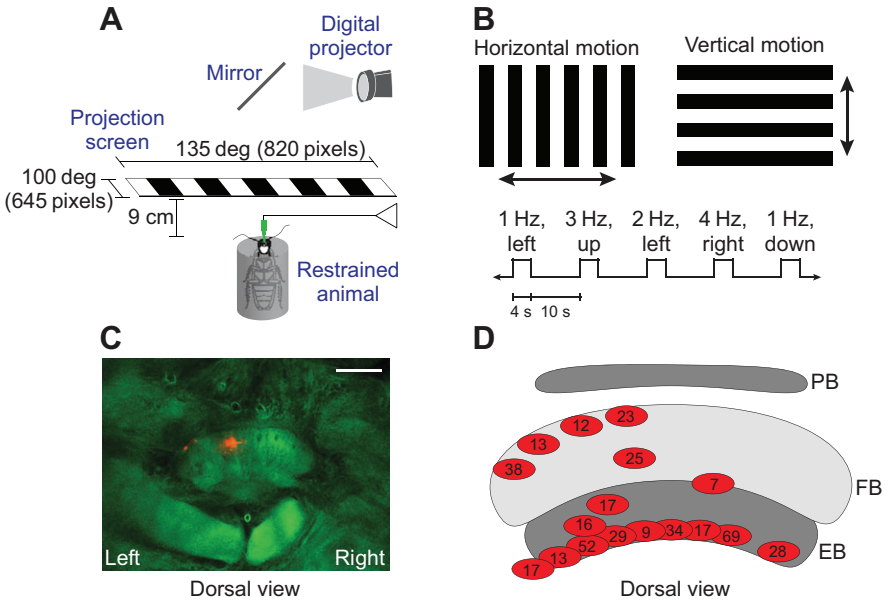

Fig. 2. Visual stimulus description and recording site locations. (A) Schematic of experimental set-up for electrophysiological recordings of animals. (B) Depiction of the stimulus at the two orientations used. Below the two stripe fields is an example of a series of trials with randomized temporal frequency, orientation and direction. Deflections from baseline only indicate the times of initiation and termination of motion. (C) Optical section of the CX with DiI indicating recording probe tracks (orange) in the left center and left margin of the fan-shaped body (FB). Scale bar is 200 µm. (D) Positions of all recording sites for visual motion experiments, indicating position at the approximate depth of the recording site and the number of units recorded from that position. Many ellipses represent multiple recordings which sampled the same location. EB, ellipsoid body; PB, protocerebral bridge.

To identify more representative temporal patterns occurring in these units, we used a fuzzy *k*-means algorithm that clustered the responses into common subgroups. We first normalized the firing rate of each response between 0 and 1. The clustering algorithm then separated the units based on temporal properties (Fig. 3). Responses in clusters with broad positive or negative changes that occurred throughout the stimulus were classified as tonic. Those with narrow peaks or nadirs were classified as phasic and grouped according to their relative location within the stimulus period. Three consistent phasic patterns were identified in this way: peaks or nadirs at the beginning, or peaks at the end of the stimulus.

Once the unit responses were placed into consistent groupings, we could examine the actual peaks and nadirs of each response within a group to identify exactly where a significant response occurred relative to baseline (described in Materials and methods). We then tested these more precise temporal response periods for significance from baseline (paired *t*-test, $P<0.05$). Responses in the tonic groups were tested over the entire stimulus period, while phasic groups were more restricted (see below). This analysis yielded 210 of 401 units (52%) with significant responses in a representative temporal pattern of the cluster they were assigned. While the remaining 58 motion-sensitive units that did not meet these additional criteria may represent important responses patterns, they occurred rarely enough that we did not consider them further in our analysis.

With this temporal information, we could then describe the phasic response characteristics quantitatively. Units responding with phasic excitation and inhibition to the initiation of motion had median response durations of 0.45 and 0.50 s, respectively (Fig. 3F), but units with phasic excitatory responses to termination had a median response duration of 1.73 s. The first quartile for these responses was at 0.60 s, similar to the initiation phasic responses. This reflects the high variability in the distribution of these termination responses. The median response delay of phasic excitation to initiation, phasic inhibition to initiation, and phasic excitation to termination were 0.15, 0.20 and 0.48 s, respectively.

Unit response types and directional selectivity

The analysis described above allowed us to classify units according to common response types that varied across visual stimulus parameters. Individual units displayed consistent response types for a given direction. For each unit we determined a standard response time interval (described in Materials and methods) then compared responses to left and right motion. Seventy-nine of 210 responding units (38%) were directionally selective to motion along the horizontal axis (two-sample *t*-test, $P<0.05$, for respective response period). These units consistently showed significantly higher mean firing rates in one direction. The response in the non-preferred direction was reduced significantly (Fig. 4A), eliminated (Fig. 4B) or depressed below baseline levels (Fig. 4C). Sixty percent of directional units were biased to the left, and 40% to the right. Units were only classified as directional if they had similar response periods, i.e. directionality was not established for units with tonic activity in one direction paired with a phasic response in the opposite direction (Fig. 4D).

Fig. 4E shows the distribution of units with regard to response types and direction. Most units (93%) maintained their tonic or phasic properties irrespective of direction. For instance, 62 units were tonic-excitatory in both directions. Sixteen of those units had a right-preferred direction, seven units had a left-preferred direction, and 39 were not directionally selective (Fig. 4E, row 2, column 2). Only five units responded phasically in one direction and tonically in the other (Fig. 4D). Among those with phasic responses, no units responded to initiation in one direction and termination in the other, or vice versa. Baseline firing rates for each unit class were variable (supplementary material Fig. S1). Histological analysis revealed no patterns relative to directional selectivity. Indeed, various units from the same recording site would often select for different directions or different phasic and tonic response properties.

Sensitivity to stimulus temporal frequency

We also examined the sensitivity of individual units to various other visual parameters. One hundred and sixty-eight units from five animals were tested with motion of at least 10 different temporal frequencies between 0.25 and 5 Hz, in both the left and right directions. There were several changes in response properties as temporal frequency varied. Twenty-six units changed from tonic responses at low frequencies to phasic responses at higher frequencies, typically over a narrow range between 1.5 and 2.5 Hz (Fig. 5). The reverse change never occurred. Interestingly, frequency effects often occurred (22 units) only in responses to one direction of movement (14 units had changes in responses to left movement

The Journal of Experimental Biology (2014) doi:10.1242/jeb.112391

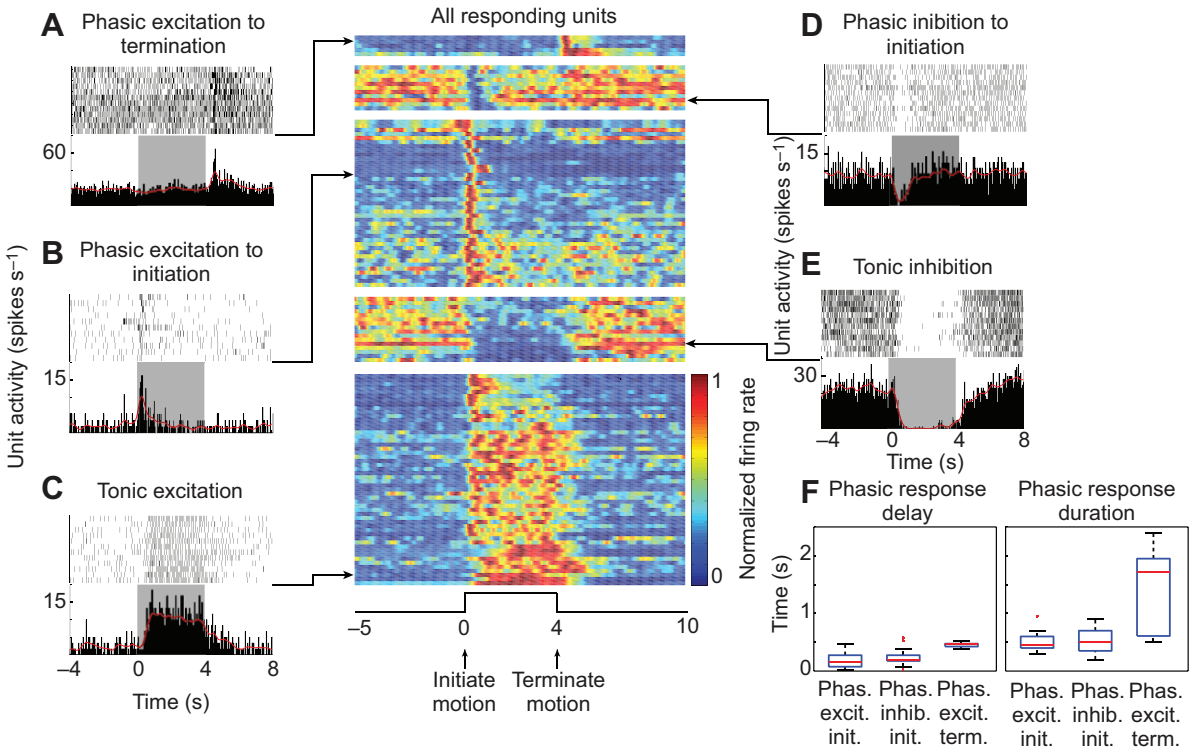

Fig. 3. Temporal properties of wide-field motion responses. Responses to wide-field visual motion had variable temporal properties that related to specific features of the stimulus. To determine what temporal response patterns were present, all unit responses (when firing rate was 2σ above or below baseline) were sorted based on their normalized mean firing rate over time (by fuzzy *k*-means clustering, binned at 50 ms) into five temporal response types. These types included responses lasting the entirety of motion (tonic) as well as brief responses (phasic) that corresponded to either the initiation or termination of motion. In all temporal classifications, with the exception of termination, responses were found as both increases and decreases of activity (excitatory and inhibitory, respectively). The heatmap in the center of the figure shows a response (normalized mean firing rate aligned to the initiation of motion, *t*=0) from each unit (rows) in the dataset, grouped by response type. (A–E) Selected unit responses as examples for each response type (indicated by arrows to the appropriate row in the heatmap). These displays include a raster plot of neural activity from each trial as well as a peristimulus time histogram (PSTH, binned at 50 ms). In each PSTH the red line represents mean firing rate (smoothed with Gaussian kernel, σ=150 ms) of all trials. The gray box on each PSTH indicates the time when stripes were moving. (F) Box and whisker plots of the means of both the response delay from stimulus onset (left) and response duration (right) for responses for each unit with phasic responses (phasic excitation to initiation, phasic inhibition to initiation, and phasic excitation to termination; *N*=58, 12 and 5). Red lines represent medians, blue boxes represent first and third quartiles, and black whiskers are the extreme data points, excluding outliers. Outliers (red +) are points greater than 1.5 times interquartile range. Phas., phasic; excit., excitation; inhib., inhibition; init., to initiation of motion; term., to termination of motion.

and eight for right movement). They included both excitatory and inhibitory responses.

Temporal frequency could also affect the directional bias of a unit. To examine this effect, we selected 93 units with significant responses that retained consistent phasic versus tonic properties across all frequencies. We then identified units that showed some significant differences in response properties as frequency varied (ANOVA, $P<0.05$) (50 units). These units were pooled and sorted by fuzzy *k*-means clustering and binned by mean response to each frequency (Fig. 6A,B). Of these units, 15 had responses that varied across frequencies only for motion in the left direction, 17 had responses that only varied for motion in the right direction, and 18 had responses that varied for both directions of motion. Our analysis revealed four clusters found from responses to left motion and five from right motion, representing variably tuned response curves to temporal frequency. Of the four average curves for responses to left motion, two (clusters 1 and 2) were of inhibitory responses and two (clusters 3 and 4) were of excitatory responses. These groupings were tuned to different ranges of temporal frequencies, distinguished by the range that evoked the strongest responses. For example, units in cluster 3 had the strongest responses at low frequencies, while the units in cluster 4 had stronger responses at higher frequencies. Similar relationships could be found in clusters with inhibitory responses. Right motion data had three clusters that were similar to left motion (1, 4 and 5) and two (2 and 3) that were more restricted to lower frequencies.

An examination of individual unit response to various temporal frequencies shows that directional selectivity could vary with temporal frequency. Units with relatively broad tuning curves for each direction maintained their directional selectivity (two-sample *t*-test, $^{\ddagger}P<0.05$, $^{*}P<0.005$) at all frequencies (Fig. 7A,B), along with units with relatively narrow curves that were similar in each direction (Fig. 7C,D), but variation in frequency tuning for different directions of motion could lead to directional selectivity only over discrete frequency ranges (Fig. 7E,F). Narrow regions of directional bias across frequencies could also occur where units showed steadily increasing responses with frequency for one direction while maintaining consistently higher responses for the other direction (Fig. 7G). Some units had less stereotypical curves, sometimes with narrow bands of reduced or increased responses that led to narrow bands of directional selectivity across frequencies (Fig. 7H). The unit depicted in Fig. 7H failed to differentiate direction at a narrow frequency band around 1.5 Hz but consistently did so at frequencies above and below this band. Moreover, since the various stimuli were presented randomly 12–15 times at each parameter combination over the entire test procedure, the gap in directionality did not come

The Journal of Experimental Biology (2014) doi:10.1242/jeb.112391

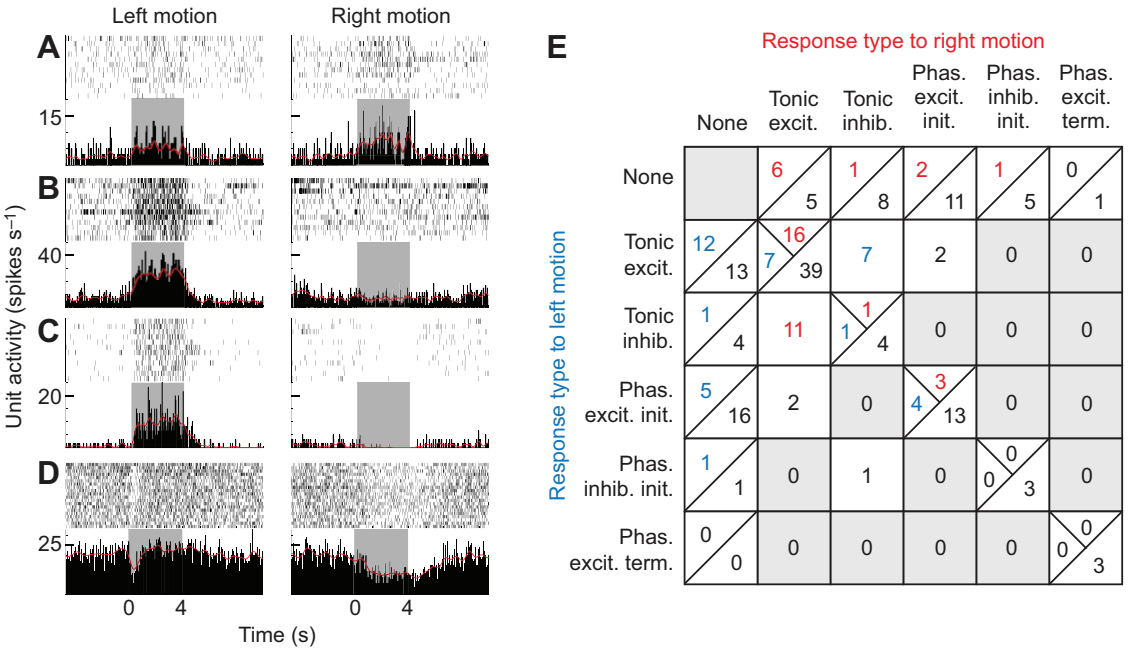

Fig. 4. Distribution of temporal response types and directional selectivity. Directional selectivity was seen in different forms, either: (A) reduced response in the null direction, (B) a loss of response in the null direction, or (C) as directional opponency (excitation in one direction and inhibition in the other). Five units were phasic in one direction and tonic in the other (e.g. D). (E) Table gives the number of units for each type of directional response. Sixty percent of directional units were biased to the left (blue numbers), and 40% to the right (red numbers). Black numbers represent units that were not directional. Preferred direction was determined as that with the higher mean firing rate for respective response period. Units with different response periods were not classified as directional. Gray shaded boxes indicate pairs of response types with no representative units. Response type abbreviations: Phas., phasic; excit., excitation; inhib., inhibition; init., to initiation of motion; term., to termination of motion.

about as a result of a transient change in responsiveness, but rather occurred whenever the ineffective frequencies were presented.

When taken in concert, a population of cells with this type of temporal frequency tuning can display different patterns of directionality depending on the temporal frequency used (Fig. 7I). Clearly, these properties emphasize the necessity to consider a range of stimulus properties before labelling a neuron as either directional or non-directional. For example, in the data depicted in Fig. 7I (all units from one experiment), a test relying solely on 1 Hz stimulation (yellow box) would generate very different results from one taken with 1.75 Hz (red box) or 3 Hz stimulation (green box).

Responses to wide-field motion with periodic firing

In 92 of 401 units tested with wide-field motion (23%), we observed periodic firing rate changes that entrained to the temporal frequency of the stimulus (Fig. 8A). Responses were classified as periodic if their spike phase distribution, relative to the temporal period of the stimulus, was non-uniform (Hodges–Ajne non-parametric test, $P<0.01$). These units often displayed distinct responses to changes in light intensity (Fig. 8B). Seventy-two percent of these units had a phasic response to either ambient light turning on, off, or both, often followed by a period of depressed activity. Bursts of spikes in these units were synchronized to a particular phase of the stripe cycle (determined by the angular mean of the spike phase distribution), yet this phase changed with frequency (Fig. 8C). Individual units were often tuned to different phases at a given frequency (offset) or with different phase-frequency relationships (slope). For one unit the phase tuning progressed linearly with frequency for stripes moving to the right (linear regression, slope=79.84), but stayed entrained to the same phase, regardless of frequency, with left moving stimulation (slope=4.85) (Fig. 8D).

No trends were seen between preferred phase or phase-frequency relationships and recording site location. These units were excluded from the cluster analysis and all analysis that relied on response type determined from the clustering. Moreover, entrained responses were rarely directionally selective and no units were entrained in one direction and not in the other.

Responses to vertical wide-field motion

Responses to vertical motion, in either direction, were far less prevalent or consistent. Only 14 of 74 units (18%) tested with vertical stimuli showed responses to motion. Of those 14 units, 13 also responded to horizontal motion. Of the 13, six had consistent tonic responses to horizontal motion, yet responses to vertical motion were inconsistent (Fig. 9). Increases in firing rate occurred randomly during the stimulus presentation, giving inconsistent response times, both across motion trials of the same stimulus parameters as well as other motion parameters. Although some of these units showed a statistical change from baseline, the response onset and duration changed for each stimulus condition and often was not in the defined response envelope from the cluster analysis. An additional six of the 13 units showed periodic activity to both horizontal and vertical motion (similar to Fig. 8). The remaining horizontal and vertical motion responding unit was phasically excited to right motion onset only. During vertical motion, it was phasically excited with upward motion only. The unit that only responded to vertical motion also only responded phasically to the onset of upward motion.

DISCUSSION

Central complex neurons convey diverse wide-field motion information

Diverse visual motion information is encoded by the neurons of the CX. Responses to the stimuli provide timing information about the initiation, termination and duration of the motion, as well as

The Journal of Experimental Biology (2014) doi:10.1242/jeb.112391

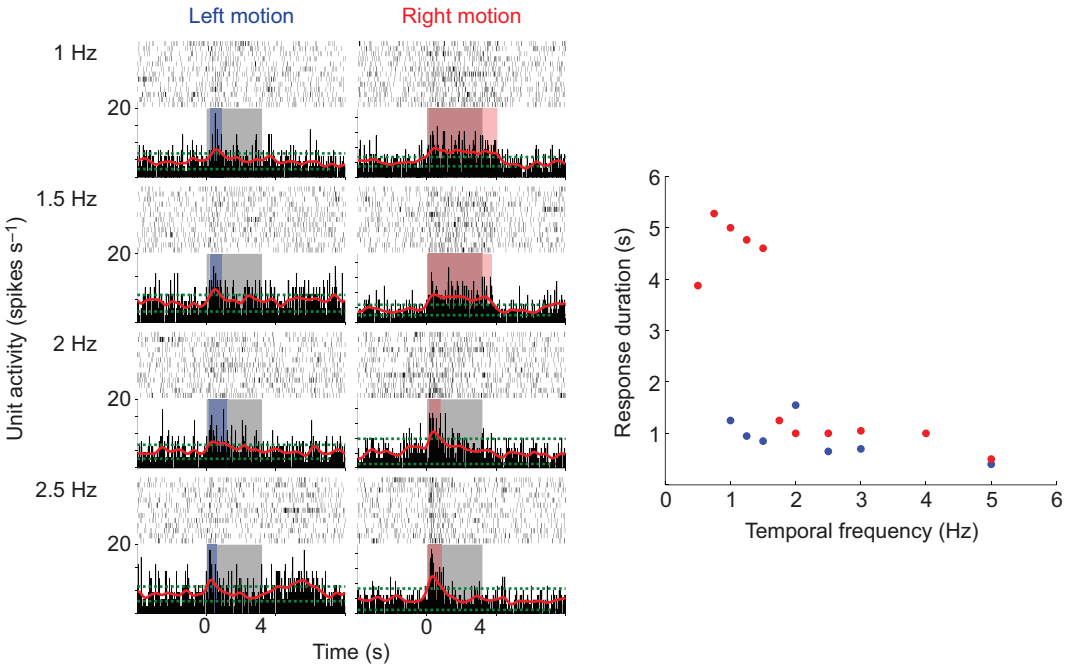

Fig. 5. Changes in response duration with temporal frequency. An example of one unit with variable response duration with temporal frequency of stimulus (in Hz) for one direction only. For each histogram, the gray box represents the time of stimulus motion. Blue (left motion) and red (right motion) boxes represent the response duration, defined by when the smoothed firing rate (red line) exceeded 2σ of the baseline (green dashed lines). Plot on the right displays response width for each temporal frequency tested for both directions (blue for left motion, red for right motion). No data points are shown if no significant response was found (e.g. there was no significant response to left motion at 0.5, 0.75, 1.75 and 4 Hz). A short response duration (indicating phasic response) is seen in all conditions except right motion of frequencies below 1.75 Hz, where the responses are tonic.

direction and temporal frequency. These units can work in concert with one another as a population of numerous cells with numerous tuning properties. Information represented in these units, such as timing of onset and/or offset of motion, as well as direction and frequency, would be useful for evoking many visually directed behaviors, such as the optomotor response. Given that these units are simply a representative sample of a large population of neurons in the CX, variations in the magnitude of these responses associated with different parameters of the stimulus may provide subtle changes of input to downstream motor control circuits.

One of the striking features of our data is that individual units are tuned to a wide range of stimulus parameters but that their response characteristics can change with certain other parameters. For example, responsiveness of the population can vary with the temporal frequency of the moving stripe field. Some broadly tuned units responded equally well over most of the frequency range that was tested (e.g. Fig. 6B, cluster 4), while others showed significant responses to a narrower band of frequencies (e.g. Fig. 6B, clusters 2, 3 and 5). Moreover, the frequency band that generated significant responses varied among units. Finally, these curves could shift, and

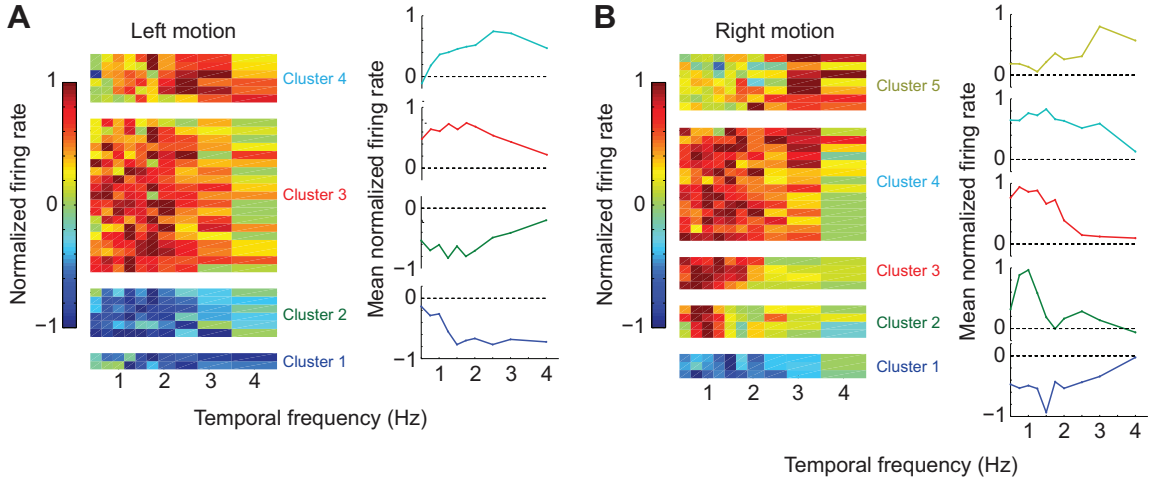

Fig. 6. Temporal frequency response curves. (A,B) Groups of similar unit response curves to temporal frequency were identified for each direction of motion (A, left; B, right). To classify response curves, unit responses that vary with frequency (ANOVA, $P<0.05$) were normalized between 1 and −1 for each frequency, pooled and sorted by fuzzy *k*-means clustering for each direction of motion (heatmaps). The mean normalized response curve for each cluster was plotted in the color of the cluster label (right of heatmaps).

The Journal of Experimental Biology (2014) doi:10.1242/jeb.112391

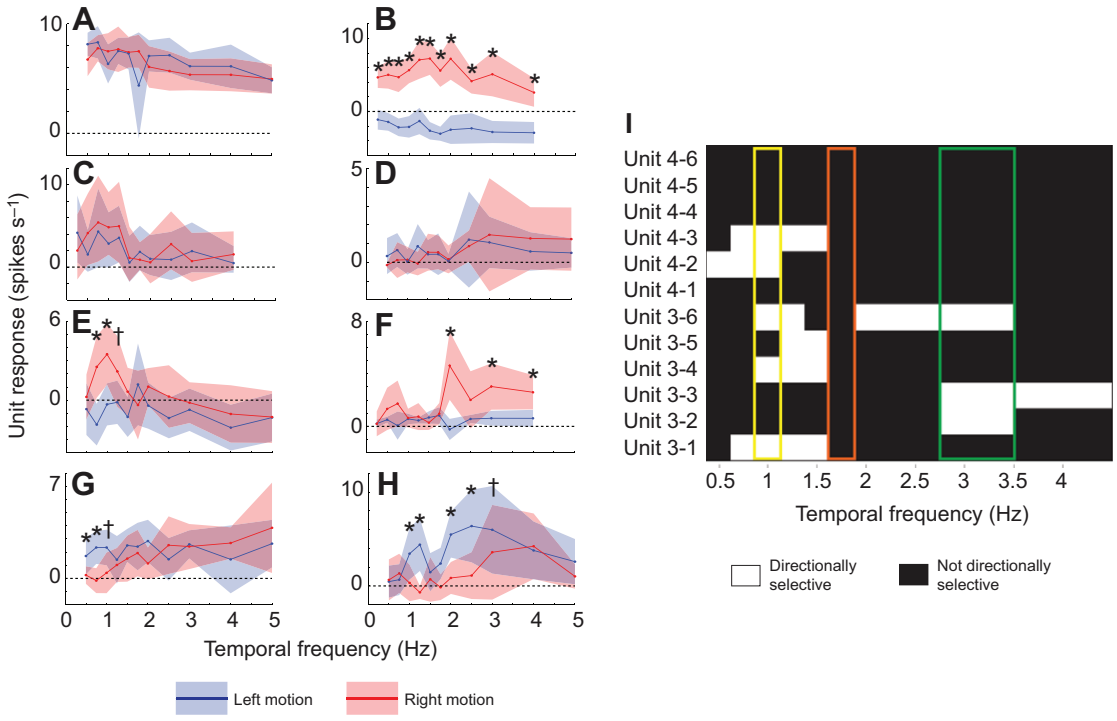

Fig. 7. Sensitivity to direction could vary with temporal frequency. (A–H) Examples of response curves of individual units, for both left (blue) and right (red) motion. Each line represents mean difference in firing rate of response period from baseline for 12–15 trials of that frequency ± standard deviation (shading). Responses to left and right motion were significantly different (two sample *t*-test, †$P<0.05$, *$P<0.005$) at various frequencies. (I) Directional selectivity of all units (rows) over a range of temporal frequencies (columns) from one recording (two tetrodes) with non-periodic motion responses. White grid cells indicate that the unit is directionally selective at that frequency ($P<0.05$), black cells indicate it is not selective. Three highlighted frequencies show different distributions of selective units. The yellow box shows that five units were directionally selective at 1 Hz, the orange box shows that no units were selective at 1.75 Hz, and the green box shows that three units were selective at 3 Hz (two are different units than those selective at 1 Hz).

become broader or narrower with other parameters like direction. Therefore, response characteristics of these units, such as directional selectivity and temporal frequency tuning, can be dependent upon one another.

We also observed varying responses to different stripe orientations. Far fewer units responded to the stripe field moving vertically, and those that did respond rarely showed a consistent pattern. This could represent a behaviorally relevant bias to horizontal motion. It is worth noting that previous work has shown a shift in response properties of CX units when cockroaches were induced to climb objects, which is visually represented as vertical motion (Guo, 2014). An alternate explanation is that the temporal frequency range for vertical motion responses is different from that for horizontal motion responses, and our stimuli fell outside the preferred range.

Periodic responses to wide-field motion

Many units displayed periodic firing entrained to the temporal frequency of the stimulus. It is likely that these units were responding to stripe features or light intensity changes rather than wide-field motion. This is supported by the strong phasic light intensity responses of many of these units. Retinotopically arranged feature detector neurons have been previously described in the fly CX (Seelig and Jayaraman, 2013). Like the rest of the units described here, no spatial correlations of recording site were found with periodic response properties. Further testing would need to be done to verify whether these units have small receptive fields, as hypothesized, and whether those units were topographically organized. In addition, the periodic units tested for vertical motion responded similarly to both orientations, unlike all other response types tested with vertical motion. This also would suggest that at least some of these units are small field light intensity detectors.

The linear changes in mean response phase are most likely to represent a fixed latency. Therefore, as the frequency of the stripe field progressed, the temporal entrainment would progress as well. Differences in slope, between units, as well as within individual units but to different directions, probably represent different latencies.

Responses similarities with motion processing neurons upstream from the central complex

The diversity of responses seen here and in other studies suggests a convergence of sensory inputs, supported by the anatomy of the region (Strausfeld, 1999). It is likely that many of the motion responses we report are processed in the optic lobes and integrated in the CX with other visual responses, as well as those of other sensory modalities. Many units displayed tonic, directionally selective, and variable temporal frequency responses to the stimuli. This is similar to the responses of motion-sensitive neurons in the periphery, such as the lobula plate tangential cells (LPTC) of the fly (Borst and Haag, 2002). LPTCs connect to thoracic motor centers, via descending neurons, as well as other brain areas, and are involved in visual course control during flight (Heisenberg et al., 1978; Geiger and Nässel, 1981; Haikala et al., 2013). LPTCs can be grouped by a preference to two orientations: horizontal (HS) and vertically (VS) sensitive cells. A functional bias to HS cells could also relate to the orientation bias in our CX cells.

The visual interneurons of the fly also have an initial transient peak of firing rate before the activity settles to a steady state at high

The Journal of Experimental Biology (2014) doi:10.1242/jeb.112391

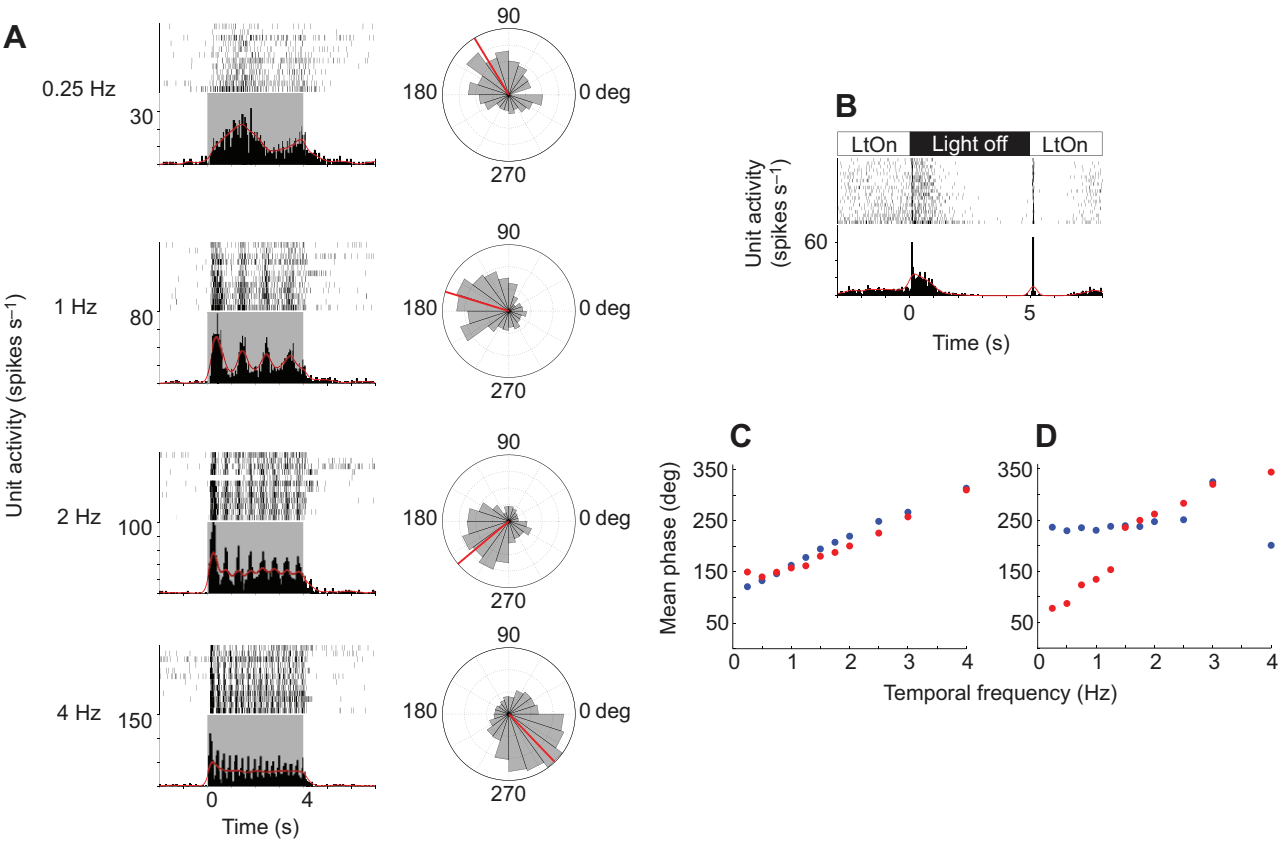

Fig. 8. Periodic responses to temporal frequency. (A) One unit response to four different temporal frequencies (in Hz) of motion. The gray box in the PSTH represents the stimulus time interval. Circular histograms to the right depict the spike distribution (binned at 18 deg of the stimulus temporal period) of the same trials as their adjacent PSTH, with 0–360 deg representing the temporal period of the stimulus, starting from the onset of motion. All four frequency distributions are non-uniform (Hodges–Ajne test, $P<0.01$), but responding to different phases of the stimulus (red line is the angular mean of the spike phases). (B) The unit had transient phasic excitation for ambient light turning on (LtOn), followed by inhibition; and a strong but longer phasic excitation to ambient light turning off; also followed by inhibition. (C) The relationship of the mean phase of the unit from the responses in A with temporal frequency of the stimulus in different directions (red=right, blue=left). The relationships were similar for each direction (linear regression, left motion: slope=52.47; right motion: slope=45.82). (D) Phase–frequency relationship of another unit with different slopes for each direction (linear regression, left direction: slope=79.84; right direction: slope=4.85).

temporal frequencies (Egelhaaf and Borst, 1989; Reisenman et al., 2003). A similar velocity effect is seen in some CX units in this study, where units with tonic responses to slower stimuli changed to phasic responses for faster stimuli. In flies, this transient spiking is only seen in relatively high temporal frequencies and is always coupled with a velocity-sensitive steady-state response at lower frequencies, which is not the case for most phasic units in this study.

Additionally, transients occurring only at the cessation of motion (Fig. 1A) are not, to our knowledge, characteristic of LPTC neurons. This distinction could also help explain the difference in response duration of these responses (Fig. 3F). We suspect that some of these responses may be after-excitation from a weak or obscured tonic inhibition. Similar durations of increased firing rate were observed anecdotally in some tonic inhibitory units after the motion ended. Units with these rebounds were rare and had varying durations, and, therefore, were not separated via clustering.

The role of central complex circuits in optomotor responses

To establish a link between the representations of wide-field motion found in the CX and sensorimotor behaviors, we described the effects of disrupting the CX on a visually directed behavior. The reversible reduction of optomotor response with procaine injection implies some role for this structure in conveying this information to motor regions. Although other systems have been described as critical, and possibly sufficient, to regulate behaviors such as optomotor response (Haikala et al., 2013), in this study we found that the CX is necessary to this behavior. It is likely that the information from the CX is not limited to involvement in optomotor behavior, yet it does play a role in this more basic, highly conserved response.

The implications of these findings do not exclude other pathways used in optomotor response, independent of the CX. At least two models for the role of the CX in sensorimotor behaviors exist. One consists of a serial pathway that includes the CX. In this model, peripheral sensory structures collect and process information that converges at the CX for further processing and integration, and is then relayed to motor regions in the thoracic ganglia. The serial nature of this model is consistent with the observation that silencing CX neurons reversibly blocks optomotor responses. Whether the CX circuits serve to create descending commands based upon visual information or modify them as they pass through, they represent a bottleneck and must be active to allow visual signals to descend from the brain. An alternative model involves parallel pathways that convey primary sensory information to both motor circuitry as well as associative regions, such as the CX. Under this model, the direct sensorimotor pathway yields fast commands based on specific sensory conditions, while the CX monitors conditions within and surrounding the animal, then modifies descending commands appropriately.

The Journal of Experimental Biology (2014) doi:10.1242/jeb.112391

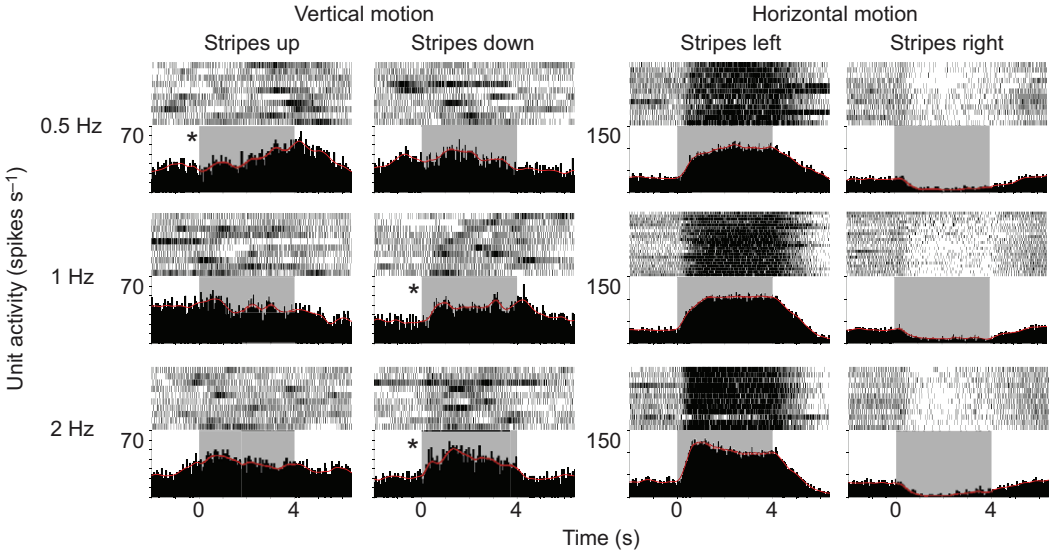

Fig. 9. Responses to vertical motion. The response of one unit to three temporal frequencies (in Hz) moving vertically (left two columns) and horizontally (right two columns). Although three conditions (*) statistically showed a response to the stimulus (paired *t*-test, $P<0.05$), response periods greatly varied across conditions, unlike the responses to horizontal motion. This property was seen in all tonic responding units that also responded to vertical motion.

This parallel model is similar to circuits seen in the basal ganglia of mammals (Alexander et al., 1991; Hikosaka et al., 2000; Kandel et al., 2013). In the mammalian motor system, direct pathways project from the motor cortex to spinal tracts or, in the case of the oculomotor system, the superior colliculus, but a parallel pathway through the basal ganglia influences the strength of those commands. Within the basal ganglia, direct and indirect pathways have opposite effects leading to the selection of appropriate behaviors at different times in the animal's experience. Those pathways rely heavily upon inhibitory connections that are altered by neuromodulators such as dopamine. Interestingly, a recent meta-analysis strongly suggests that the CX is deeply homologous to the mammalian basal ganglia (Strausfeld and Hirth, 2013). Moreover, the CX is heavily invested in GABAergic (inhibitory) receptors as well as receptors for numerous neuromodulators, including dopamine (Homberg et al., 1999; Kahsai and Winther, 2011; Kunst et al., 2011; Kahsai et al., 2012).

Under the parallel model, it is not as clear why silencing the CX would block optomotor responses or other behaviors (Ridgel and Ritzmann, 2005; Harley and Ritzmann, 2010). A possible explanation is that the role of the CX is so critical that some baseline activity is necessary for the direct pathways to express any behavior (Hikosaka et al., 1993). In either model the CX circuits can have profound effects on the optomotor response or any other behavior. Taking advantage of the large amounts of sensory information available to them as well as the rich supply of neuromodulators within the CX, they could play an important role in adjusting the insect's behaviors to match the internal and external context on a moment-to-moment basis. This ability to rapidly adapt to changing conditions is, indeed, a hallmark of animal behavior that easily distinguishes it from more static reflexive behavior.

MATERIALS AND METHODS

Animals

Adult male cockroaches, *Blaberus discoidalis* Serville 1839, were used in all experiments. Animals were housed in 5-gallon buckets, given food and water *ad libitum*, and kept on a 12 h:12 h light:dark cycle at 27°C. Recordings and behavioral testing typically began 2–3 h into the dark cycle.

Animal preparation and electrophysiology

Animals were anesthetized with ice and wings were removed. For extracellular recordings, a thread tourniquet was tied loosely around the neck, tight enough to reduce hemolymph flow but not so tight as to damage neck connectives. Reduction of hemolymph flow was necessary, because continued flow to the head results in a large clot forming over the brain, making it difficult to target specific regions. The insect was placed in a vertical plastic tube (Fig. 2A), and held in place with cork and wax to fill the spaces in the tube. A plastic plate was fixed with wax on top of the tube and the head was fixed to the plate with wax across the mouthparts and behind the head, with negligible visual occlusion. A small portion of the cuticle between the ocelli was removed, with some connective and fatty tissue, to expose the ventral surface of the brain. Care was taken to avoid damage to the ocellar nerve or optic tracts. Saline (Tryba and Ritzmann, 2000) added to the head cavity just covered the brain tissue. A copper reference electrode was inserted into the mesothoracic spiracle. After the experiments the animals typically walked normally.

Prior to insertion in the brain, the two shanks of the 16-channel silicon probes (NeuroNexus A-series 2×2 tetrodes, Ann Arbor, MI, USA) were dipped 5–10 times in DiI paste (Invitrogen NeuroTrace CM-DiI Paste, Eugene, OR, USA) for fluorescent labelling of the electrode tracks. Each shank is 15 µm thick and 150 µm apart from center to center, and contains two diamond-shaped iridium recording site tetrodes, also spaced 150 µm apart vertically from center to center. The impedance of each channel was 2–3.5 MΩ. The probe was mounted on the headstage of the Neuralynx Cheetah32 digital data acquisition system (Bozeman, MT, USA) and driven into the brain with a micromanipulator. Unit activity was sampled at 30.3 kHz and band-pass filtered between 600 and 6000 Hz. Only recording waveforms exceeding a predetermined voltage threshold for any channel of the tetrode were saved.

Visual stimuli

All visual stimuli were generated with a custom graphics program written in Python utilizing the OpenGL graphics library (provided by John Bender). Visual stimuli generated at 75 frames s^{-1} were displayed by a PLUS UA-1080 DLP projector, lit with a mercury arc lamp with a UV filter, projecting onto a screen 9 cm from the animal that subtended 135 deg horizontally and 100 deg vertically, centered on the frontal visual field, resulting in a resolution of 820×645 pixels (Fig. 2A). The wide-field motion stimuli consisted of a shifting, sharp edged, black and white stripe field, covering the entire screen (Fig. 2B). Each trial consisted of the stripe field shifting for

a duration of 4 s with some combination of parameters, varied randomly between trials (Fig. 2B). The varied parameters were temporal frequency, orientation and direction. The temporal frequencies tested were 0.25, 0.5, 0.75, 1.0, 1.25, 1.5, 1.75, 2.0, 2.5, 3.0, 4.0 and 5.0 Hz. Only two orientations were tested: vertically oriented stripes that shifted horizontally (horizontal motion) and horizontally oriented stripes that shifted vertically (vertical motion). Each orientation shifted in both directions, left/right and up/down, respectively. After a 6–10 s latent period, the stripe field would shift again for the next trial. Repeated parameter sets occurred randomly throughout the experiment so that, for example, all 20 trials of 0.25 Hz motion to the right direction did not repeat sequentially over a brief time period, but were presented randomly across the entire recording period. The stripes had a Michelson contrast of 0.96 calculated with luminances of 53.7 cd m^{-2} (white stripe) and 1.1 cd m^{-2} (dark stripe) measured with a Pentax Spotmeter V (TI Asahi, Saitama, Japan) and were 33° wide (therefore the stripe field had a spatial wavelength of 66°). Contrast and width were held constant across all trials for all conditions.

To verify that the refresh rate of the stimuli was sufficient, four animals were tested with an analog display system. Neural responses were compared for various stimulus parameters and were found to have no significant differences from the digital system (supplementary material Fig. S2). Stimulus timing was synchronized to neural data with direct transistor–transistor logic (TTL) output from the stripe generator for digital trials and from a photodiode during analog trials.

For behavior trials, the animal was facing an LCD monitor (NEC LCD17-BK, Tokyo, Japan), driven at 60 Hz with a spatial resolution of 1280×1024 pixels. The monitor was positioned 12 cm from the animal's head and subtended 110 deg horizontally and 110 deg vertically, centered on the frontal visual field. The stripes had a Michelson contrast of 0.97, calculated with luminances of 71.6 cd m^{-2} (white stripe) and 1.1 cd m^{-2} (dark stripe). The stripe field parameters were held constant at 2 Hz temporal frequency and 66° spatial wavelength, moving horizontally for 10 s. Only direction was altered, which was randomly alternated between trials.

Spike sorting and analysis

Spike data from each tetrode were sorted off-line into unit clusters. Automated spike sorting was first performed using KlustaKwik (version 1.5; K. Harris, Rutgers University, as part of the MClust toolbox, version 3.5; A. D. Redish, University of Minnesota), which utilizes an expectation–maximization algorithm to separate spikes by the waveform parameters peak and energy (L2 norm). Cluster selection was very conservative, discarding units that had greater than 2% of its spikes with less than 100 ms inter-spike interval or units that did not maintain separation throughout the experiment. Great lengths were taken to get accurate cluster separation over these long recording periods. All waveforms were examined over time and manually corrected using Offline Sorter (Plexon Inc., Dallas, TX, USA), which is excellent at visualizing waveform parameters over time. In addition, approximately five trials (1 Hz temporal frequency, both in the left and right direction), were compared from the beginning and end of each experiment. If any significant change in response was observed, in magnitude or timing, the unit was discarded.

After unit sorting, spike times were imported into MATLAB (The MathWorks, Natick, MA, USA), where all further data analysis was performed. Unit responses to particular parameter sets of stimuli were shown with peristimulus time histograms (PSTH), calculated by binning spikes into 50 ms bins and convolving that histogram with a Gaussian kernel (σ=150 ms) to estimate instantaneous firing rate.

For temporal response patterns and response curve classification, a fuzzy *k*-means clustering algorithm was used, with a fuzzy factor of 1.5 (based on code from J. M. Fellous, University of Arizona). Fuzzy *k*-means clustering is a weighted clustering algorithm derived from a standard *k*-means clustering, which identifies cluster centers and determines the Euclidean distance for each data point to each of the centers. Standard *k*-means clustering assigns the data points to one and only one of *k* number of clusters. The fuzzy *k*-means clustering algorithm, however, assigns a probability to each data point of belonging to each one of the clusters and therefore may belong to two or more clusters (for details, see Fellous et al., 2004). This is an optimal clustering algorithm when few data points are available, as standard *k*-means clustering may lead to a large number of local minima. For temporal response patterns, the parameters used for clustering were the normalized peristimulus firing rates, at 50 ms intervals from 5 s before the beginning of the stimulus to 5 s after the end of the stimulus period. Mean firing rates were normalized between 0 and 1 by subtracting the minimum firing rate and dividing by the maximum rate.

Once response temporal patterns were established via clustering, individual response times were defined for each unit response. Responses for phasic units were determined by searching for peaks or nadirs within a time range defined for that response type. This search period was defined by the stimulus and the response envelope for that cluster (two standard deviations after the mean response time). Response period was determined by half of the peak/nadir height from mean baseline firing rate. For instance, for a unit response in the cluster of 'phasic initiation – excitatory', a peak was found between 0 and 0.2 s (the response envelope for that cluster) from stimulus onset. A period of 0 to 0.5 s was used to search for phasic responses to ambient light changes. The response period was then determined by the width of the response peak at half its height from baseline. Tonic response periods were simply the stimulus period. This response period was used for significance testing against the baseline (paired two-tailed *t*-test, comparing the spike counts of the time periods divided by duration of the time periods of each trial) to verify a response of that type. In addition, a standard response period for a unit was found if the unit had only one response type across a given parameter, such as direction. This period was used for response comparisons (two-sample two-tailed *t*-test, also comparing the spike counts of the time periods divided by duration of the time periods of each trial) across different stimulus parameters, such as temporal frequency. The standard response period was determined by the minimum and maximum response periods of all responses of that given type for that unit.

An ANOVA test was also used to identify units with variable responses across different temporal frequencies to be included in tuning curve classification. For response curves to temporal frequency, the parameters used for clustering were normalized differences of mean firing rate for that unit's standard response period from baseline. These differences were normalized between −1 and 1 by subtracting the minimum absolute value of the differences and dividing them by the maximum difference. For both instances, *k* was selected based on pair-wise cluster separation statistics and visual assessment. Clusters with two or less units were merged with the closest cluster.

Behavioral testing

Healthy male animals were tethered onto a 15.24 cm air-supported Styrofoam ball that was monitored by optical mouse sensors and recorded by a customized MATLAB program (Guo and Ritzmann, 2013). Two trials were performed before injection to assess the animal's ability to perform an optomotor response. Animals that did not walk or noticeably display the response were discarded. After injection of either procaine or saline (N=15, 15 animals, respectively), the animal was placed back on the tether. Behavior was monitored every 15 min (recording ball movements for 90 s, with one visual motion trial 30 s into the trial) for a total of 60 min (five total trials). After 60 min, the animal was removed from the ball and we then observed the animal during free walking and noted any abnormal behaviors.

The occurrence of an optomotor response was indicated when: (1) the mean angular turning velocity during the stimulus was mean ± 2 s.e.m. of the turning velocity for 10 s before the stimulus and (2) the mean turning velocity was in the same direction of the stimulus. Significant differences between treatment and control groups were found using a Pearson's χ^2 test.

Procaine injection

Pretested animals were removed from the ball and injected using single barrel capillary tubes (World Precision Instruments, outer diameter/inner diameter 1.0/0.58 mm), pulled to a large tip size (700c, DKI Vertical Puller, Tujunga, CA, USA), which was then scored and broken so the new tip was between 20 and 40 µm outer diameter. These pipettes were backfilled with either a procaine solution or cockroach saline. Procaine hydrochloride 99% (Acros Organics AC20731) was dissolved to 20% and

10% concentrations, both in saline and 2% dextran fluorescein (Invitrogen D1822). Procaine, a sodium channel blocker, has been shown to reversibly inhibit neural activity in insect brains (Müller et al., 2003; Devaud et al., 2007). Animal preparation was identical to restrained electrophysiology protocols above, except the brain was de-sheathed. The solution was injected into the central brain, frontally, using a PM 2000 (B) 4-channel pressure injection system (Microdata Instrument Inc, South Plainfield, NJ, USA). After the experiment, injection volumes were estimated by injecting the solution into white petrolatum. Estimated injection volumes averaged 2.07±1.8 nl. Two controls were performed, a saline injection and a sham consisting of an identical surgery but with no injection. After the injection or sham, the neck tourniquet was removed and the head capsule was sealed.

For electrophysiological testing of procaine-injected brains, the animal was prepared identically to the previous restrained recording preparations. The only exception was that the brain was de-sheathed before the recording electrodes were inserted. After recording was initiated and some units were roughly identified, a baseline was recorded for 5−10 min. The injection pipette was then carefully lowered into the central brain at ~45 deg from vertical (to fit both injection and recording apparatus in the available space). If previously identified units still remained, the procaine or saline solution was then injected into the brain (at the same specifications as behavior trials). Recordings then persisted for approximately an hour after injection. All further recording and spike sorting procedures were identical to previously discussed methods.

Histology and imaging

At the end of both neural and behavioral experiments, brains were dissected from the animals, fixed in 4% paraformaldehyde, rinsed in 0.1 mol l^{-1} phosphate buffer solution, dehydrated in an increasing ethanol series, and cleared with methyl salicylate. The entire brain was then mounted in DPX mounting medium and optical sections were taken coronally using a confocal microscope (LSM700, Zeiss, Oberkochen, Germany) and ×10 objective. No physical sectioning was needed, as the 400−500 µm thick tissue samples were imaged from both sides. Autofluorescence of the neural structures was used to identify the location of either the DiI-lined electrode tracks (Fig. 2C) or the injected procaine-dye mixture (Fig. 1C,D).

Acknowledgements

We thank Dr John Bender for providing Python and MATLAB software along with advice in experimental design and analysis, Dr Josh Martin for providing MATLAB software along with advice on analysis, Dr Jean-Marc Fellous for providing MATLAB software, and Alan Pollack for assistance with equipment, histology, and microscopy, and for maintaining the cockroach colonies.

Competing interests

The authors declare no competing financial interests.

Author contributions

N.D.K. designed, performed and analyzed all data from electrophysiological experiments, performed histological and confocal analysis, and led the preparation of the manuscript. M.K. designed, performed and analyzed all data from the behavioral procaine experiments. R.E.R. provided input to the interpretation of the data and contributed to the final version of the manuscript.

Funding

This work was supported by the National Science Foundation (IOS-1120305 to R.E.R.).

Supplementary material

Supplementary material available online at
http://jeb.biologists.org/lookup/suppl/doi:10.1242/jeb.112391/-/DC1

References

Alexander, G. E., Crutcher, M. D. and DeLong, M. R. (1991). Basal ganglia-thalamocortical circuits: parallel substrates for motor, oculomotor, 'prefrontal' and 'limbic' functions. *Prog. Brain Res.* **85**, 119-146.

Bausenwein, B., Müller, N. R. and Heisenberg, M. (1994). Behavior-dependent activity labeling in the central complex of *Drosophila* during controlled visual stimulation. *J. Comp. Neurol.* **340**, 255-268.

Bender, J. A., Pollack, A. J. and Ritzmann, R. E. (2010). Neural activity in the central complex of the insect brain is linked to locomotor changes. *Curr. Biol.* **20**, 921-926.

Borst, A. and Haag, J. (2002). Neural networks in the cockpit of the fly. *J. Comp. Physiol. A* **188**, 419-437.

Borst, A., Haag, J. and Reiff, D. F. (2010). Fly motion vision. *Annu. Rev. Neurosci.* **33**, 49-70.

Devaud, J.-M., Blunk, A., Podufall, J., Giurfa, M. and Grünewald, B. (2007). Using local anaesthetics to block neuronal activity and map specific learning tasks to the mushroom bodies of an insect brain. *Eur. J. Neurosci.* **26**, 3193-3206.

Egelhaaf, M. and Borst, A. (1989). Transient and steady-state response properties of movement detectors. *J. Opt. Soc. Am. A* **6**, 116-127.

Fellous, J.-M., Tiesinga, P. H. E., Thomas, P. J. and Sejnowski, T. J. (2004). Discovering spike patterns in neuronal responses. *J. Neurosci.* **24**, 2989-3001.

Geiger, G. and Nässel, D. R. (1981). Visual orientation behaviour of flies after selective laser beam ablation of interneurones. *Nature* **293**, 398-399.

Guo, P. (2014). *The Role Of The Central Complex In Adaptive Locomotor Behavior In Cockroaches*. PhD dissertation, Case Western Reserver University, Cleveland, OH, USA.

Guo, P. and Ritzmann, R. E. (2013). Neural activity in the central complex of the cockroach brain is linked to turning behaviors. *J. Exp. Biol.* **216**, 992-1002.

Guo, P., Pollack, A. J., Varga, A. G., Martin, J. P. and Ritzmann, R. E. (2014). Extracellular wire tetrode recording in brain of freely walking insects. *J. Vis. Exp.* **86**, e51337.

Haikala, V., Joesch, M., Borst, A. and Mauss, A. S. (2013). Optogenetic control of fly optomotor responses. *J. Neurosci.* **33**, 13927-13934.

Harley, C. M. and Ritzmann, R. E. (2010). Electrolytic lesions within central complex neuropils of the cockroach brain affect negotiation of barriers. *J. Exp. Biol.* **213**, 2851-2864.

Heinze, S. and Reppert, S. M. (2011). Sun compass integration of skylight cues in migratory monarch butterflies. *Neuron* **69**, 345-358.

Heisenberg, M., Wonneberger, R. and Wolf, R. (1978). optomotor-blind H31 – a *Drosophila* mutant of the lobula plate giant neurons. *J. Comp. Physiol. A* **124**, 287-296.

Hikosaka, O., Matsumura, M., Kojima, J. and Gardiner, T. (1993). Role of basal ganglia in initiation and suppression of saccadic eye movements. In *Role of the Cerebellum and Basal Ganglia in Voluntary Movement* (ed. N. Mano, I. Hamada and M. DeLong), pp. 213-219. Amsterdam: Elsevier.

Hikosaka, O., Takikawa, Y. and Kawagoe, R. (2000). Role of the basal ganglia in the control of purposive saccadic eye movements. *Physiol. Rev.* **80**, 953-978.

Homberg, U., Vitzthum, H., Müller, M. and Binkle, U. (1999). Immunocytochemistry of GABA in the central complex of the locust *Schistocerca gregaria*: identification of immunoreactive neurons and colocalization with neuropeptides. *J. Comp. Neurol.* **409**, 495-507.

Huber, F. (1960). Untersuchungen über die funktion des zentralner-vensystems und insbesondere des gehirns bei der fortbewegung und lauterzeugung der grillen. *Z. Vgl. Physiol.* **44**, 60-132.

Kahsai, L. and Winther, Å. M. E. (2011). Chemical neuroanatomy of the *Drosophila* central complex: distribution of multiple neuropeptides in relation to neurotransmitters. *J. Comp. Neurol.* **519**, 290-315.

Kahsai, L., Martin, J.-R. and Winther, A. M. E. (2010). Neuropeptides in the *Drosophila* central complex in modulation of locomotor behavior. *J. Exp. Biol.* **213**, 2256-2265.

Kahsai, L., Carlsson, M. A., Winther, A. M. E. and Nässel, D. R. (2012). Distribution of metabotropic receptors of serotonin, dopamine, GABA, glutamate, and short neuropeptide F in the central complex of *Drosophila*. *Neuroscience* **208**, 11-26.

Kandel, E., Schwartz, J. and Jessell, T. (2013). *Principles of Neural Science*. 5th edn. New York, NY: McGraw-Hill.

Kunst, M., Pförtner, R., Aschenbrenner, K. and Heinrich, R. (2011). Neurochemical architecture of the central complex related to its function in the control of grasshopper acoustic communication. *PLoS ONE* **6**, e25613.

Müller, D., Staffelt, D., Fiala, A. and Menzel, R. (2003). Procaine impairs learning and memory consolidation in the honeybee. *Brain Res.* **977**, 124-127.

Ofstad, T. A., Zuker, C. S. and Reiser, M. B. (2011). Visual place learning in *Drosophila melanogaster*. *Nature* **474**, 204-207.

Otto, D. (1971). Untersuchungen zur zentralnervösen Kontrolle der Lauterzeugung von Grillen. *Z. Vgl. Physiol.* **74**, 227–271.

Pfeiffer, K. and Homberg, U. (2014). Organization and functional roles of the central complex in the insect brain. *Annu. Rev. Entomol.* **59**, 165-184.

Phillips-Portillo, J. (2012). The central complex of the flesh fly, *Neobellieria bullata*: recordings and morphologies of protocerebral inputs and small-field neurons. *J. Comp. Neurol.* **520**, 3088-3104.

Poeck, B., Triphan, T., Neuser, K. and Strauss, R. (2008). Locomotor control by the central complex in *Drosophila* - an analysis of the tay bridge mutant. *Dev. Neurobiol.* **68**, 1046-1058.

Reisenman, C., Haag, J. and Borst, A. (2003). Adaptation of response transients in fly motion vision. I: Experiments. *Vision Res.* **43**, 1291-1307.

Ridgel, A. L. and Ritzmann, R. E. (2005). Effects of neck and circumoesophageal connective lesions on posture and locomotion in the cockroach. *J. Comp. Physiol. A* **191**, 559-573.

Ridgel, A. L., Alexander, B. E. and Ritzmann, R. E. (2007). Descending control of turning behavior in the cockroach, *Blaberus discoidalis*. *J. Comp. Physiol. A* **193**, 385-402.

Ritzmann, R. E., Ridgel, A. L. and Pollack, A. J. (2008). Multi-unit recording of antennal mechano-sensitive units in the central complex of the cockroach, *Blaberus discoidalis*. *J. Comp. Physiol. A* **194**, 341-360.

Rosner, R. and Homberg, U. (2013). Widespread sensitivity to looming stimuli and small moving objects in the central complex of an insect brain. *J. Neurosci.* **33**, 8122-8133.
Sakura, M., Lambrinos, D. and Labhart, T. (2008). Polarized skylight navigation in insects: model and electrophysiology of e-vector coding by neurons in the central complex. *J. Neurophysiol.* **99**, 667-682.
Seelig, J. D. and Jayaraman, V. (2013). Feature detection and orientation tuning in the *Drosophila* central complex. *Nature* **503**, 262-266.
Strausfeld, N. J. (1999). A brain region in insects that supervises walking. *Prog. Brain Res.* **123**, 273-284.
Strausfeld, N. J. (2012). *Arthropod Brains: Evolution, Functional Elegance, and Historical Significance*. Cambridge, MA: Harvard University Press.
Strausfeld, N. J. and Hirth, F. (2013). Deep homology of arthropod central complex and vertebrate basal ganglia. *Science* **340**, 157-161.
Strauss, R. (2002). The central complex and the genetic dissection of locomotor behaviour. *Curr. Opin. Neurobiol.* **12**, 633-638.
Szczecinski, N. S., Brown, A. E., Bender, J. A., Quinn, R. D. and Ritzmann, R. E. (2014). A neuromechanical simulation of insect walking and transition to turning of the cockroach *Blaberus discoidalis*. *Biol. Cybern.* **108**, 1-21.
Triphan, T., Poeck, B., Neuser, K. and Strauss, R. (2010). Visual targeting of motor actions in climbing *Drosophila*. *Curr. Biol.* **20**, 663-668.
Tryba, A. K. and Ritzmann, R. E. (2000). Multi-joint coordination during walking and foothold searching in the *Blaberus* cockroach. I. Kinematics and electromyograms. *J. Neurophysiol.* **83**, 3323-3336.
Weir, P. T., Schnell, B. and Dickinson, M. H. (2014). Central complex neurons exhibit behaviorally gated responses to visual motion in *Drosophila*. *J. Neurophysiol.* **111**, 62-71.

The Journal of Experimental Biology